УДК 691.175
Тарек Эльсаед – доцент
E-mail: elsayedtarek@hotmail.ru
Хешам Хаггаг – старший преподаватель
Авад Ель Хашими – старший преподаватель
Ахмед Хассан – ассистент
Инженерный факультет Хельванского университета, Матария, Каир, Египет

ПОВЕДЕНИЕ ПЛИТ, УСИЛЕННЫХ КВАДРАТНОЙ СТЕКЛОПЛАСТИКОВОЙ СТЕРЖНЕВОЙ АРМАТУРОЙ

АННОТАЦИЯ

Коррозия стальной арматуры – один из наиболее серьезных недостатков армированного бетона. Для очистки железобетонных конструкций от коррозии необходимы огромные усилия и большие материальные затраты. Использование стеклопластиковой арматуры взамен стальной является разумным решением проблемы коррозии. Статья посвящена исследованию оптимального использования стеклопластиковой арматуры в укреплении плит. Проведен сравнительный анализ и по результатам испытаний даны рекомендации.

КЛЮЧЕВЫЕ СЛОВА: квадратная арматура, стеклопластиковая арматура, полипропиленовые волокна, плиты.

Tarek Elsayed – associate professor
Hesham Haggag – assistant professor
Awad El Hashimy – assistant professor
Ahmed Hassan – assistant lecturer
Faculty of Engineering, Mataria, Helwan University, Cairo, Egypt

BEHAVIOR OF SLABS REINFORCED USING SQUARE GFRP REBARS

ABSTRACT

Corrosion of steel bars is a common problem encountered in steel reinforced concrete structures. The repair of steel corrosion costs a lot of money and time. The use of fiber-reinforced polymers (FRP) reinforcing bars instead of steel rebars is a reasonable solution of the corrosion problem. In this paper, a study was made to enhance the behavior of slab specimens reinforced using GFRP rebars. The parameters included in this study were, the geometry of bar cross-section, the characteristic strength of concrete, reinforcement percentage, and the percentage of polypropylene fibers in the concrete mixtures. Test specimens were nine, one-way, slabs. The study revealed that reinforcing one-way slabs in this research using GFRP rebars, square in croess-section, is effective in enhancing slabs` failure mode, cracking and ultimate loads, and deflections than using GFRP rebars circular in cross-section. Test results were analyzed and compared together and the corresponding conclusions and recommendations regarding the behavior and design of such slabs were drawn.

KEYWORDS: Square rebars, GFRP rebars, Polypropylene fibers, slabs.

INTRODUCTION

Over the last years, research has been conducted in order to find solutions for the corrosion problem of steel reinforced concrete. As a result, methods such as galvanization, the use of stainless steel bars, cathodic protection and epoxy coatings has been tried. None of these remedies has proved to be completely efficient. The excellent properties of fiber-reinforced polymers (FRP) suggested that these materials might be the solution for corrosion resistant materials reinforcing concrete. These properties include high resistance to corrosion, high strength-to-weight ratio and fatigue resistance [1]. Most FRP structural applications in engineering fall into two areas. The first involves replacing steel reinforcing bars with carbon fiber reinforced polymer (CFRP), glass fiber reinforced polymer (GFRP) or aramid fiber reinforced polymer (AFRP). The second application is to strengthen structurally deficient slabs with

FRP sheets or plates. The application of these materials in large scale has been delayed due to the high cost of FRP reinforcement in comparison to steel, due to the lack of design codes and due to the brittle behavior of FRP, resulting in poor structural ductility. To secure composite action, sufficient bond must be mobilized between reinforcement and concrete for fulfillment of full transfer of forces from one to the other. However, the shape of the cross section determines the bonded area and, hence, affects the bond behavior. A. Chillides, Pilakoutas and Waldron (1996) [2] reported that square bars develop higher bond strength than round bars under full confinement conditions.

RESEARCH SIGNIFICANCE

In this work, behavior of concrete slabs reinforced with GFRP rebars with different cross-section geometry was studied. The study considered the parameters those may enhance the behavior of tested slabs. The research included a comparison between GFRP reinforced slabs with similar slabs manufactured using steel reinforced concrete. The study is expected to contribute to the following outcomes

- Understanding the behavior of concrete slabs reinforced with GFRP rebars, with different geometry of cross-sections.
- Encouraging the use of GFRP, reinforcing rebars in reinforced concrete structures.
- Reducing repair cost of new reinforced concrete structures and redirect this money in other activities.

EXPERIMENTAL INVESTIGATION

One-way reinforced concrete slabs reinforced with steel and GFRP rebars were investigated. The variables considered included the geometry of the cross-section of the reinforcing GFRP rebars, circular and square, the characteristic strength of concrete, 25, 35, and 45 N/mm^2 (3570, 5000, 6429 psi), polypropylene fiber content in concrete mixes, zero, 1.5, and 2.5 kg/m^3 (zero, 0.1, and 0.17 lb/cft). Nine slab specimens were included in this research.

Manufacturing GFRP bars

The GFRP reinforcing square bars used in this research were manufactured using mechanical pultrusion process. The pultrusion process is one of the most cost-effective methods for the production of composite materials. A continuous process produces constant cross section parts. Fig. 1 shows a schematic diagram of the process of pultrusion of GFRP bars. After manufacturing the bars, they were left for enough time to set, and then the corners of the square bars were machined to smooth curved shape in order to eliminate the concentrated stresses at the bars corners. Bars were then wrapped helically by fiber yarns in 1 cm pitch to roughen their surfaces.

a)

b)

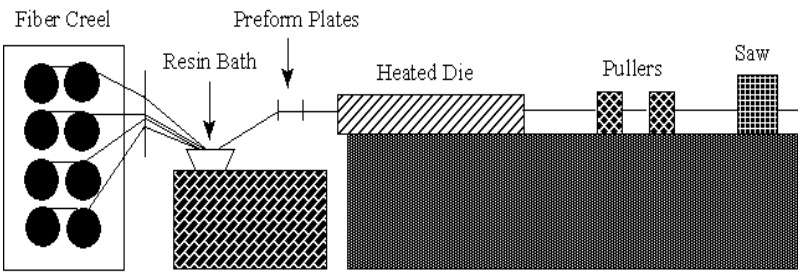

Fig. 1. Pultrusion process of GFRP-square rebars:
a – The pultrusion machine; b – schematic diagram of the pultrusion process

Table 1

Tensile strength of the manufactured GFRP rebars

Specimen Number	Dimensions, mm (in.)	Ultimate Tensile Strength, N/mm^2 (psi)	Average Ultimate Strength, N/mm^2 (psi)
1	14x14 (0.55x0.55)	607.143 (86735)	602.228 (86033)
2	14x14 mm (0.55x0.55)	602.041(86005)	
3	14x14 mm (0.55x0.55)	597.5 (85357)	
4	Æ16 (0.63)	592.5 (84643)	582.5 (83214)
5	Æ 16 (0.63)	575 (82143)	
6	Æ 16 (0.63)	580 (82857)	

Table 2

Bond strength of the manufactured GFRP rebars

Group	Specimen	Bars			P.P kg/m^3 (lb/cft)	Fcu N/mm^2 (psi)	Failure Load kN (lb)	Bond Strength M/mm^2 (psi)	Average Bond Strength N/mm^2 (psi)
		Type	Dim. mm (in.)	Wrapping pitch					
I	P1	Steel	Æ 16 (0.63)	-	Zero	28.30 (4042.87)	68.2 (15038)	4.511 (645)	4.478 (640)
	P2	Steel	Æ 16 (0.63)	-	Zero	28.30 (4042.87)	67 (14774)	4.445 (635)	
II	P3	GFRP	Æ 16 (0.63)	Smooth	Zero	28.30 (4042.87)	29 (6395)	1.924 (275)	1.94 (277)
	P4	GFRP	Æ 16 (0.63)	Smooth	Zero	28.30 (4042.87)	29.5 (6505)	1.957	
	P5	GFRP	Æ 16 (0.63)	1 cm (0.4 in.)	1.5 (0.1)	27.50 (3928.58)	57.6 (12701)	3.82 (546)	3.81 (544)
	P6	GFRP	Æ 16 (0.63)	1 cm (0.4 in.)	1.5 (0.1)	26.30 (3757.16)	57.2 (12613)	3.8 (543)	
	P7	GFRP	Æ 16 (0.63)	1 cm (0.4 in.)	2.5 (0.17)	27.50 (3928.58)	62 (13671)	4.113 (588)	4.146 (592)
	P8	GFRP	Æ 16 (0.63)	1 cm (0.4 in.)	2.5	2630 (3757.16)	63 (13892)	4.18 (597)	
III	P9	GFRP	14x14 (0.55x 0.55)	Smooth	Zero	28.30 (4042.87)	33 (7277)	1.964 (281)	1.958 (280)
	P10	GFRP	14x14 (0.55x 0.55)	Smooth	Zero	28.30 (4042.87)	32.8 (7232)	1.952 (279)	
	P11	GFRP	14x14 (0.55x 0.55)	1 cm (0.4 in.)	1.5 (0.1)	29.00 (4142.87)	65 (14333)	3.87 (553)	3.884 (555)
	P12	GFRP	14x14 (0.55x 0.55)	1 cm (0.4 in.)	1.5 (0.1)	28.30 (4042.87)	65.5 (14444)	3.898 (557)	
	P13	GFRP	14x14 (0.55x 0.55)	1 cm (0.4 in.)	2.5 (0.17)	27.50 (3928.58)	71 (15656)	4.226 (604)	4.285 (612)
	P14	GFRP	14x14 (0.55x 0.55)	1 cm (0.4 in.)	2.5 (0.17)	27.50 (3928.58)	73 (16097)	4.345 (620)	

Materials

The fiber volume fraction used in manufacturing the GFRP bars was taken 56 %. This ratio is the optimum and it also matching the range recommended by ACI-440 [3]. The fibers used in manufacturing the GFRP bars are E-glass fibers with linear weight of roving 2400 g/km, and the used resin is polyester E.S 1319 mixed with cobalt in the ratio 1000:1, by weight. This ratio gives a setting time of about 2 hours at 160 єC (320 єF) which is enough for manufacturing process. The manufactured GFRP rebars used in this research were tested under tensile load to estimate their behavior under axial tension. The bond strength between the rebars and concrete was also tested. Table 1, and table 2 represents the results of tensile and pullout tests respectively.

Specimens

The experimental program includes testing nine reinforced concrete one-way slabs. All slabs had the same dimensions of 2100 mm (82.7 in.) long , 500 mm (19.7 in.) wide , and 150 mm (5.9 in.) depth as shown in Fig. 2. They were divided into five groups as presented in Table 3. The first group included one slab specimen reinforced with high tensile steel bars of yield and ultimate strengths of 360 and 520 N/mm^2 (51429, and 74286 psi) respectively, which was considered as control specimen. The other four groups were arranged in a way to include the considered parametres in this research.

Table 3

Details of the experimental program

Group	Slab No	No of bars in specimen	Bar shape	Bar Dimension mm (in.)	Material OF Bar	PP. content kg/m^3 (lb/cft)	Fcu N/mm^2 (psi)	Parameter studied
I	S1	3	Circular	Æ 16 (0.63)	Steel	Zero	25 (3572)	Control
II	S2	3	Circular	Æ 16 (0.63)	GFRP	1.5 (0.1)	25 (3572)	Shape of bar
	S3	3	Square	14x14 (0.55x 0.55)	GFRP	1.5 (0.1)	25 (3572)	
III	S4	3	Square	14x14 (0.55x 0.55)	GFRP	1.5 (0.1)	35 (5000)	Fcu
	S5	3	Square	14x14 (0.55x 0.55)	GFRP	1.5 (0.1)	45 (6429)	
IV	S6	4	Square	14x14 (0.55x 0.55)	GFRP	1.5 (0.1)	25 (3572)	Rfts. ratio
	S7	5	Square	14x14 (0.55x 0.55)	GFRP	1.5 (0.1)	25 (3572)	
V	S8	3	Square	14x14 (0.55x 0.55)	GFRP	Zero	25 (3572)	PP content
	S9	3	Square	14x14 (0.55x 0.55)	GFRP	2.5 (0.17)	25 (3572)	

Manufacturing specimens

Plywood forms were used in casting test slabs. Nine wooden forms were used, each specimen was cast in a separate form to ensure good quality specimens. A plastic sheet was glued to the forms to prevent the mixing water to be adsorped by the wooden form. A mechanical mixer was used to mix concrete with maximum capacity of 0.125 m^3 (4.42 cft). The use of mechanical vibrator ensured full compaction of concrete. Specimens were cured by water spraying twice a day for complete 28 days. After 28 days age, slabs were tested. Fig. 3 shows the used formwork, fig. 4 shows specimens after casting.

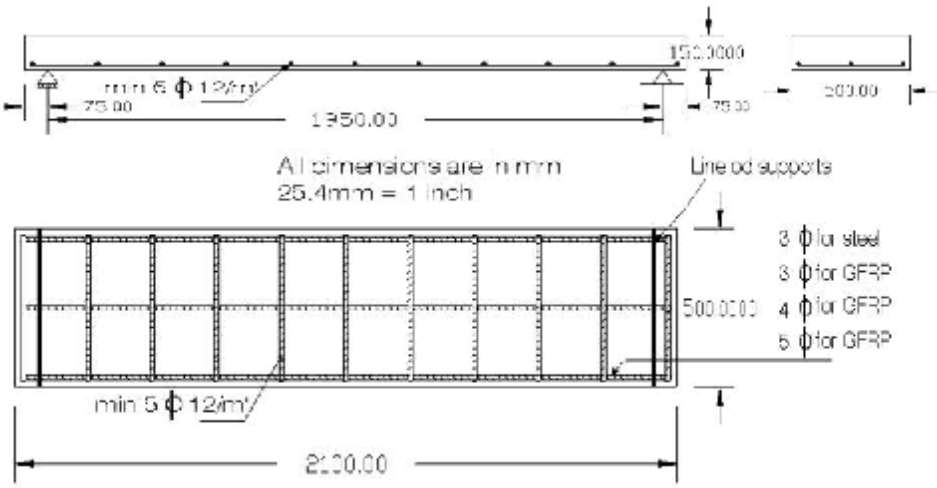

Fig. 2. Geometry and dimensions of tested slabs

Fig. 3. Used Formwork

Fig. 4. Cast specimens

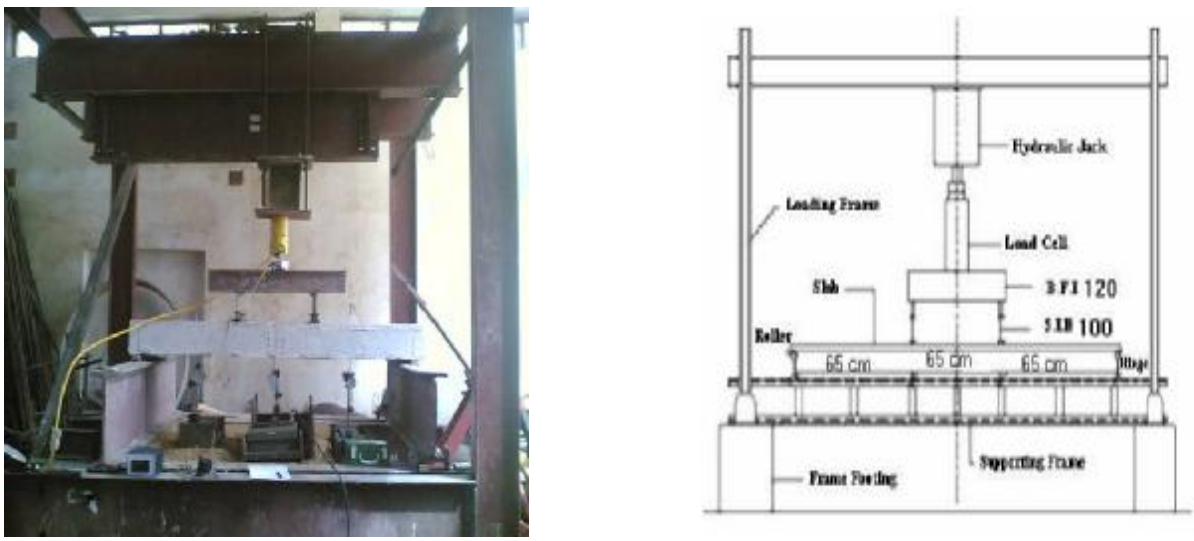

Fig. 5. Test setup

Test setup and instrumentations

Test specimens were placed in the loading frame in the Materials testing laboratory in the Faculty of Engineering Mataria, Helwan University, Egypt. The specimens were simply supported on two I-beams to form two line supports. The clear span between these supports was 1950 mm (76.8 in.) (fig. 2). For all test specimens, strains in longitudinal reinforcing bars were measured using electrical strain gauges, 5 mm length, electrical resistance of 119.8 ± 0.20 ohms, and gauge factor (2.11±1 %). A compression hydraulic jack of 500 kN (110230 lb) capacity was

used at the mid-span of the slab. A load cell of 300 kN (66138 lb) capacity was placed underneath the loading jack. Three I-beams were used to form two symmetric line loads on tested specimens. The loads were applied at distances of 650 and 1300 mm (25.6 and 51.2 in.) from the right support. Fig. 5 shows a general view of the test setup and loading system. Fig. 6 shows a schematic diagram of a test specimen under loading.

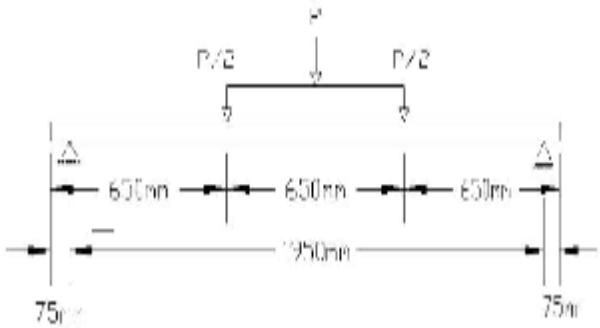

Fig. 6. Schematic diagram of test specimen

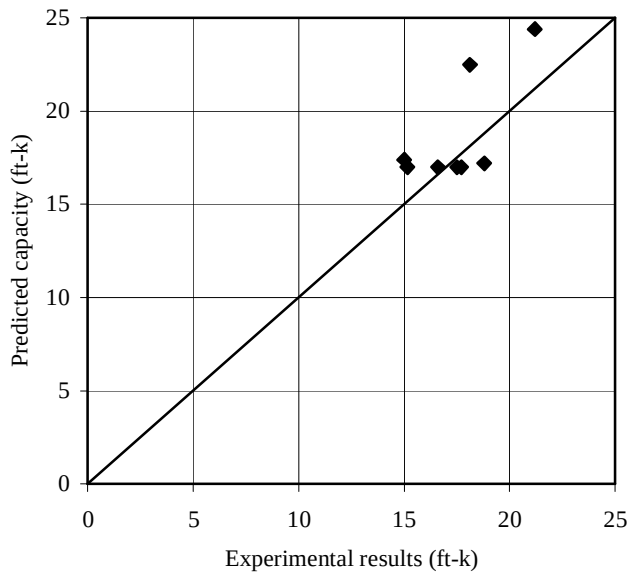

Fig. 7. Comparison of predicted under loading and experimental results (1 ft-k = 1.34 m-kn)

ANALYTICAL INVESTIGATION

The strength design philosophy for flexural strength of concrete sections reinforced with FRP bars presented in ACI-440 [3] was used for the estimation of the nominal flexural capacity of test specimens in this research. The design material properties stated in the ACI-440 [3] were followed in the analysis and the specimens were considered to be in the conditions not exposed to earth and weather, (i.e. $C_E = 0.8$). The equations used in the ACI-440 [3] are:

In case failure of the member is initiated by crushing of concrete:

$$M_n = A_f f_f (d - \frac{a}{2}) \quad (1)$$

In case failure of the member is initiated by rupture of FRP bars:

$$M_n = A_f f_{fu} (d - \frac{\beta_1 c}{2}) \quad (2)$$

Where:

M_n = nominal flexural capacity

A_f = cross-sectional area of FRP rebars

f_f = tensile stresses in the FRP rebars

f_{fu} = tensile strength of FRP rebars

a = $\beta_1 c$ = depth of the compression block of the section

d = the distance from the center of the reinforcing steel bars in tension to the extreme compression fiber of the section

Comparison of predictions and experimental results

The ACI-440 [3] includes two conditions controlling the flexural design approach of concrete section reinforced with FRP bars. These conditions are:

- a section controlled by concrete crushing is defined as section in which $\rho_f \geq 1.4\rho_{fb}$ and
- a section controlled by FRP rupture is defined as one in which $\rho_f < \rho_{fb}$

When applying these conditions in the analysis using equations (1), and (2), the predicted nominal flexural

capacities of test specimens were in a reasonable agreement with the experimental results fig. 7. This reveals that the design approach of concrete sections reinforced by FRP bars, ACI-440 [3] is suitable for predicting the nominal flexural strength of concrete slabs reinforced by FRP bars, square in cross-section similar to those tested in this research.

EXPERIMENTAL RESULTS AND DISCUSSION

In this research, the parameters included are geometry of the reinforcing bars, the reinforcement ratio, the characteristic strength, and the content of polypropylene fibers in concrete. Nine solid slab specimens, fig. 2, table 3, were tested to study the effect of the mentioned parameters on failure mode, cracking and ultimate loads, load-deflection relationship, and the load-strain in reinforcements. This will be discussed in details in the following sections. Test results are summarized in table 4.

Table 4

Results of tested slabs

Slab	S1	S2	S3	S4	S5	S6	S7	S8	S9
Reinforcement	3 Æ 16 Steel	3 Æ 16 GFRP	3 Square GFRP Bars	3 Square GFRP Bars	3 Square GFRP Bars	4 Square GFRP Bars	5 Square GFRP Bars	3 Square GFRP Bars	3 Square GFRP Bars
Fcu, N/mm^2 (psi)	25 (3572)	25 (3572)	25 (3572)	35 (5000)	45 (6429)	25 (3572)	25 (3572)	25 (3572)	25 (3572)
PP content, kg/m^3 (lb/cft)	zero zero	1.5 0.1	1.5 0.1	1.5 0.1	1.5 0.1	1.5 0.1	1.5 0.1	zero zero	2.5 0.17
AS (%)	0.79	0.79	0.79	0.79	0.79	1.045	1.31	0.79	0.79
Cracking Load, kN (lb)	52 (11464)	22 (4850)	27.8 (6129)	38.5 (8488)	41.5 (9149)	37.5 (8267)	48 (10582)	19.2 (4233)	32.2 (7099)
Ultimate Load kN (lb)	78.9 (17394)	63.8 (14065)	70.3 (15498)	74.4 (16402)	80 (17637)	77 (16975)	90 (19841)	64.4 (14198)	75.2 (16579)
Percentage of cracking to ultimate load (%)	66	34	40	52	52	48	54	29.8	43

Fig. 8. Failure mode of tested slabs:
a) Crack pattern for slab reinforced with steel rebars; b) Crack pattern for slab reinforced with 3-circular GFRP rebars;
c) Crack pattern for slab reinforced with 3-square GFRP rebars; d) Crack pattern of slab reinforced with 5-square GFRP rebars

Failure mode

Failure of all tested slabs is flexural failure characterized by initiation of cracks at the tension side within the maximum moment zone as indicated in fig. 8. Slab reinforced with steel rebars showed the traditional ductile failure mode. Fig. 8 a, figs. 8 b, c. show that using GFRP rebars with square cross-section enhances the failure mode of tested slabs as the crack spacing for slab reinforced with square rebars is slightly lesser than crack spacing observed for slab reinforced with circular GFRP rebars. Thus, the failure mode of slabs reinforced with square rebars showed better ductility than slabs reinforced with circular rebars. This is almost due to the effect of the bigger surface area and due to the slight increase in the bond strength of the square rebars when compared to those of circular rebars (table 2). Observations during tests showed that increasing the reinforcement ratio reduces the crack spacing with the increase of load and thus enhances the failure mode of tested slabs (fig. 8 d). The same behavior was observed when increasing the concrete characteristic strength. Test observations also revealed that the addition of polypropylene fibers enhances slightly the failure mode of the tested slabs. As with the addition of fibers, the mechanism of the crack formation is slightly changed [4]. Some tensile load can be transferred across the crack by the bridging of fibers, thereby; the stress in the concrete comes from not only the bond stress but the bridging of fibers as well. With the contribution from the fibers, less bond stress is needed to reach the same cracking stress. Consequently, the spacing of crack is smaller in slabs with fibers than in slabs without Fibers [4]. The reduction in crack spacing was remarkably observed for specimens manufactured with polypropylene fibers content of 2.5 kg/m^3 while the reduction in crack spacing was not remarkable for fibers content of 1.5 kg/m^3.

Cracking and ultimate loads

With reference to table 4, it is clear that slab reinforced with steel bars gave the higher cracking and ultimate loads for same reinforcement ratio and characteristic strength. It should be mentioned that steel reinforced slabs were cast without polypropylene fibers. It is clear from table 4 that GFRP rebars with square cross-section gave higher cracking and ultimate loads than those given by test specimen reinforced by circular GFRP rebars by about 25 and 10 % respectively. This may be related to the effect of the higher surface area and the higher bond strength of square rebars compared to those of circular rebars. It should be noted that the effect of the smooth finished corners of the square bars helps in improving their bond srength with concrete. It is also clear from Table 4 that the higher the characteristic strength the higher are the cracking and ultimate loads. The effect of the percentage of GFRP sqaure reinforcement on the behavior of slabs in this research was considered by testing slab specimens with reinforcement ratio 0.79, 1.045, and 1.31 %. It was estimated that for each increase of 0.255 % in the reinforcement ratio increases the cracking and the ultimate loads of tested slabs by about 35 and 14 % repectively. The effect of polypropylene fibers content on the cracking and ultimate loads of tested slabs was considered in this paper. It is shown in table 4 that adding polypropylene fibers in concrete mixes plays a significant role in enhancing the cracking loads and slightly increases the ultimate load of tested slabs. The used polypropylene fibers content is zero (for plain specimens), 1.5 and 2.5 kg/m^3 (zero, 0.1, and 0.17 lb/cft); these contents are equivalent to zero, 0.17 %, and 0.28 % of concrete volume. The increase in polypropylene fibers was noticed to be very effective in increasing the cracking load, thanks to the effect of the polypropylene fibers in changing the mechanism of crack formation as the bridging of fibers in cracks contributes in mobilizing less bond stress to reach the same cracking stress [4]. The average increase in the cracking and ultimate loads was estimated to be about 31 % and 13 % respectively.

Load – mid-span deflection

Deflections of test specimens were recorded at three points; at mid-span and the two middle points in the distance between the center and the support from each side. The load – mid-span deflection relationship was drawn for each slab at figs. 9, 10, 11, and 12. As presented in fig. 9, it is shown that slabs reinforced with square GFRP rebars showed higher flexural stiffness than slab reinforced with circular GFRP rebars. This is almost related to the effect of the higher surface area and the higher bond strength of square rebars than those for circular rebars. In addition, the smooth curved-finished corners of the square rebars improved the bond strength between the bars and concrete and consequently helped in postponing the crack initiation to higher load stages that resulted in improving specimen's flexural stiffness. The enhancement of the load-deflection relationship of slabs due to increasing concrete characteristic strength is not remarkable, fig. 10, fig. 11 shows that the higher the reinforcement area, the lower are the mid-span deflections of tested slabs. This is logic, as the increase in reinforcement area reduces the average stresses in reinforcing bars and consequently reduces the resulting strains, and this leads to higher flexural stiffness of tested slabs, and therefore, the mid-span deflection is reduced. As mentioned before, adding polypropylene fibers in concrete mixes plays a significant role in enhancing the cracking and the ultimate loads of tested slabs, thanks to the bridging effect of the polypropylene fibers in cracks of concrete that contributes in mobilizing less bond stress to reach the same cracking stress. This leads to reducing the tensile strains in the GFRP rebars and thus the mid-span

deflection are reduced, fig. 12, and consequently, the failure mode is enhanced.

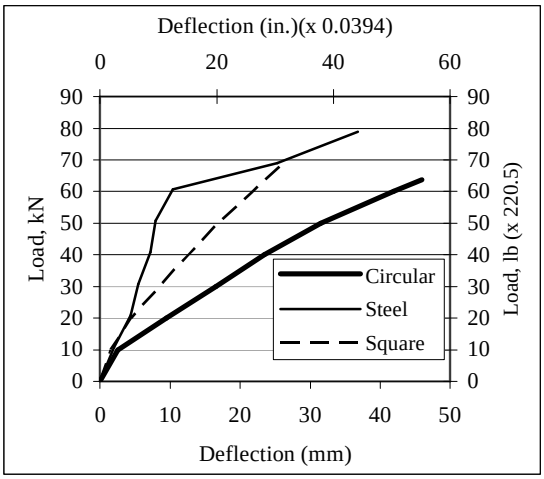

Fig. 9. Effect of bar cross-section geometry on mid-span deflection

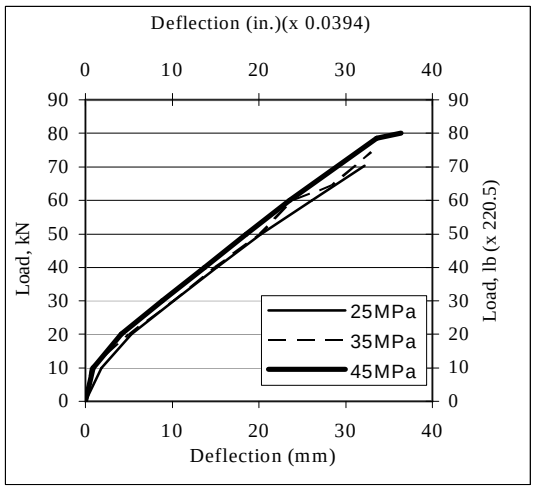

Fig. 10. Effect of characteristics strength on mid-span deflection

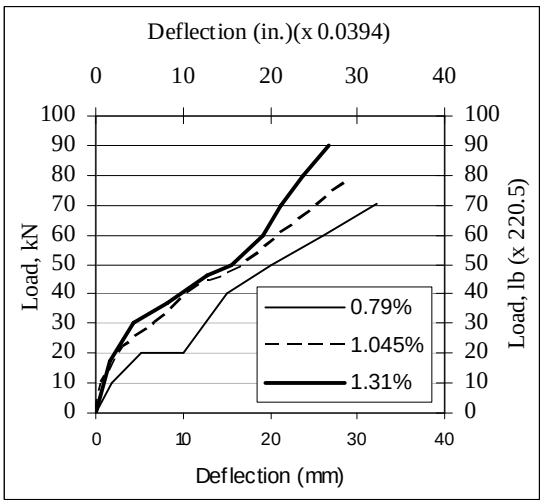

Fig. 11. Effect of percentage of reinforcement on mid-span deflection

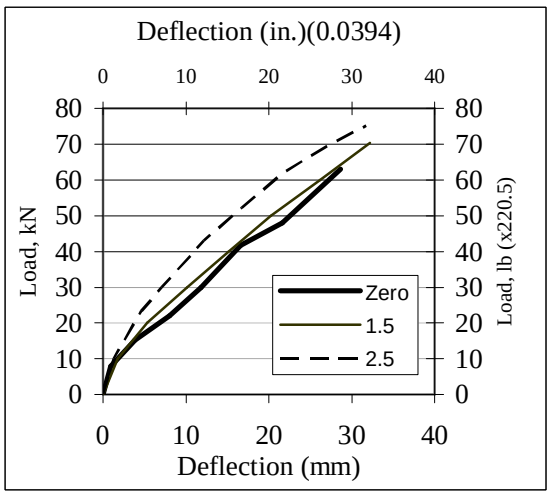

Fig. 12. Effect of polypropylene fibers content on mid-span deflection

Load-strain relationship in reinforcements

The effect of geometry of reinforcing bars, reinforcement ratio, characteristic strength, and the content of polypropylene fibers in concrete, on the load-strains relationships of tested slabs are shown in figs. 13 to 16. Fig. 13 illustrates the effect of bar cross-section geomtry on the load-strain relationships of the used rebars. The steel reinforcements showed a typical ductile behavior of steel reinforced slabs, as the load-strain relationship starts linear up to yielding and then the load-strain rate decreased due to strain hardening. The other types of reinforcing rebars are GFRP with circular and square cross-section, S2, and S3 to S9. Generally speaking, the load-strain relationships of the GFRP rebars showed higher strains compared to those of steel rebars and thus the secant modulus of the steel rebars was estimated to be about five times greater than those for GFRP rebars. On the other hand, fig. 13 showed that square GFRP rebars showed lower strains compared to those for circular GFRP rebars. The secant modulus of square GFRP rebars was estimated to be about 1.5 times greater than that for circular GFRP rebars. And thus the difference in behavior between slabs reinforced with GFRP square and circular rebars can be explained. As explained before in this research, the mid-span deflections of slabs with square rebars were lower than those for slabs rienforced with circular rebars, Thanks to the higher secant modulus and the higher bond strength of the sqaure rebars when compared to those of circular rebars. Also the higher secant modulus of the sqaure rebars resulted in lower tensile strains than those produced in the circular rebars and thus the rate of propagation of cracks and also the rate of debonding between the rebars and concrete are lower than those for slabs rienforced with circular rebars. Consquently, using square rebars in rienforcing concrete slabs in this research resulted in higher ultimate loads and

better failure mode than using circular rebars.

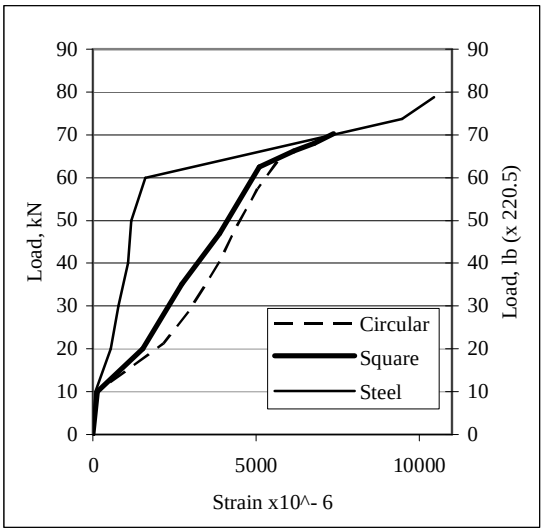

Fig. 13. Effect of bar cross-section geometry on load-strain relationship of rebars

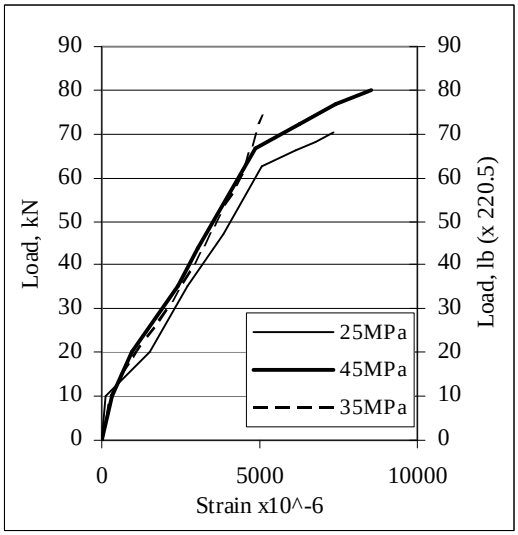

Fig. 14. Effect of characteristic strength on load-strain relationship of rebars

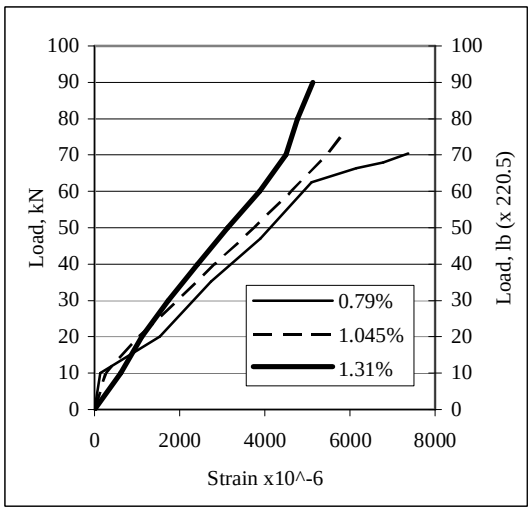

Fig. 15. Effect of percentage of reinforcement on load-strain relationship of rebars

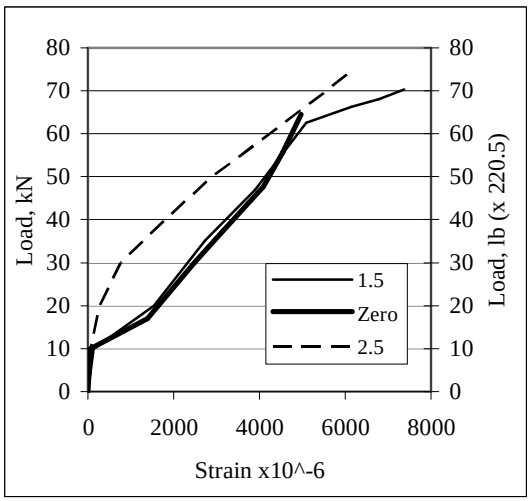

Fig. 16. Effect of polypropylene content on load-strain relationship of rebars

The load-strain relationships in fig. 14 indicates that the effect of the characteristic strength of concrete, in the range considered in this research, on the load-strain relationship is not remarkably clear, but a conclusion is still valid, the higher the charcteristic strength the lower are the strains in the reinforcing bars.

In this research, three reinforcement percentages were used for slabs reinforced with GFRP rebars, 0.79, 1.045 and 1.31 %. These reinforcement percentages were done by using 3, 4, and 5 square rebars in tested slabs. The load-strain relationships in fig. 15 represents the effect of varying reinforcement percentage of GFRP rebars on the load-strain behavior of tested specimens. It is shown in fig. 15 that the higher the reinforcement percentage the lower are the strains in GFRP rebars. This is logic as increasing the GFRP reinforcement percentage by increasing the number of rebars increases their overall cross-sectional area and thus decreasing the average tensile stress in the rebars and concequently the tensile strain decreases.

Fig. 16 shows the effect of varying the content of polypropylene fibers in concrete used in casting test specimens. It is shown in fig. 16 that adding polypropylene fibers to concrete with content up to 1.5 kg/m^3 (0.1 lb/cft), has almost nigligible effect on the load-strain behavior of the GFRP rebars. This low dosage of fibers makes the concentration of the fibers in concrete to be very low, and as described before in this research, the effect of the fibers on the behavior of test specimen is concentrated on the bridging effect of fibers in cracks. This low fiber concentration makes most of cracks to be free of fibers an thus the strains in the fiber rebars remains almost

unchanged. It is also shown in fig. 16 that, adding 2.5 kg/m^3 (0.17 lb/cft) polypropylene fibers have a remarkable effect on the load-strain of the GFRP rebars, as the strains in the rebars were remarkably reduced. This is almost attributed to the effect of the polypropylene fibers in enhancing the bond strength between concrete and the GFRP rebars as well as the contribution of fibers bridging and thus providing extra confinenment for the reinforcing bars and therefore, the tensile strains in the rebars are reduced.

FUTURE RESEARCH

It is recommended to study the controling of cracks width of concrete slabs reinforced with square GFRP rebars to increase their durability, also testing slab specimens under aggressive environment is needed.

CONCLUSIONS

In this research the behavior of one-way slabs reinforced with square GFRP rebars was studied. The pultrusion process using materials available in the loacal market manufactured the used GFRP rebars. Some parameters were considered in the study for the purpose of enhancing the behavior of slabs in this research. Test results revealed that using GFRP rebars, sqaure in cross-section, in manufacturing reinforced concrete one-way slabs in this research is effective in improving their behavior, as using square GFRP rebars instead of circular rebars enhances their failure mode, reduces the deflections, and increases their cracking and ultimate loads. The study also revealed that, adding polypropylene fibers to concrete used in casting slabs in this research, is an effective technique in improving the failure mode, mid-span deflection, ductility, and increasing the load carrying capacity of slabs reinforced with square GFRP rebars, tested in this research. Simple calculations in this research showed that the flexural strength design of concrete sections reinforced with FRP bars presented in the ACI-440 is suitable for predicting the nominal flexural strength of concrete slabs reinforced by FRP bars, square in cross-section similar to those tested in this research.

REFERENCES

1. Ferreira A.J.M., Camanho P.P., Marques A.T. and Fernandes A.A. Modelling of concrete beams reinforced with FRP re-bars. Faculty of Engineering, University of Porto, Rua dos Bragas, 4099 porto codex, Portugal, 2001.
2. Chillides Z., Pilakoutas K. and Waldron P. Anchorage Systems – Bond Improvement. Euro Crete Report № CCC/96, Centre for Cement and Concrete, The University of Sheffield, Oct. 1996.
3. American Concrete Institute (ACI). Guide for the Design and Construction of Concrete Reinforced with FRP Bars. Report by ACI Committee, 440, November 1, 2000.
4. Wang H. and Belarbi A. Flexural Behavior of Fiber-Reinforced-Concrete Beams Reinforced with FRP Rebars. ACI Materials Journal, SP230-51, Oct. 1, 2005.
5. The Egyptian Code of Practice for Designing and Executing Concrete Structures, ECP 2003-2007.
6. Hosny A.H.H., El-Nawawy O.A., Mostafa El., Khalil A.H.H. Behavior of Concrete Slabs Reinforced with Fiber-Glass Bars. The 1st Middle East Workshop on Structural Composites, Sharm El-Sheikh, Egypt, June 14-16, 1996. – PP. 267.
7. Haggag A.H., Hanna N.F., Gad R.M. Behavior of One-Way Concrete Slabs Reinforced by GFRP Rebars and Polypropylene Fibers. Engineering Research Journal, Helwan University, Faculty of Engineering, Mataria, Egypt, Vol. 85, February 2003. – PP. 59-67.
8. Ombers L., Alkhrdaji T., Nanni A. Flexural Analysis of one-way Concrete Slabs Reinforced with GFRP-Rebar's. International Meeting on Composite Materials, Plast 2000. Proceedings Advancing with Composites 2000, Milan, Italy, May 2000. – PP. 243-250.

УДК 624.012.35/45
Ф.С. Замалиев – кандидат технических наук, доцент
Р.А. Сагитов – инженер
Ш.Н. Хайрутдинов – инженер
E-mail: shamil153@mail.ru
Казанский государственный архитектурно-строительный университет

ИСПЫТАНИЕ ФРАГМЕНТА СТАЛЕЖЕЛЕЗОБЕТОННОГО ПЕРЕКРЫТИЯ НА СТАТИЧЕСКИЕ НАГРУЗКИ

АННОТАЦИЯ

Целью испытания являлось определение напряженно-деформированного состояния фрагмента сталежелезобетонного перекрытия при статических нагрузках. Приведены графики развития прогибов, деформаций сдвига на границе сталь-бетон и деформаций нижнего пояса стальных балок перекрытия.

КЛЮЧЕВЫЕ СЛОВА: сталежелезобетонные конструкции, статическая нагрузка, испытание.

F.S. Zamaliev – candidate of technical science, associate professor
R.A. Sagitov – engineer
Sh.N. Khayrutdinov – engineer
Kazan State University of Architecture and Engineering

STATIC LOAD TEST OF COMPOSITE STEEL AND CONCRETE CEILING FRAGMENT

ABSTRACT

The purpose of this test is estimation of the stress-strain mode of composite steel and concrete ceiling fragment under static load. The diagrams of deflection increase, shear strain of steel-concrete connection, and tensile strain of the bottom flange of steel beams are given.

KEYWORDS: composite steel and concrete structures, static load, test.

При реконструкции жилых и общественных зданий возникает потребность замены существующих перекрытий по деревянным балкам, не нарушая при этом статической связности зданий. Замену деревянных перекрытий в отечественной практике часто производят с помощью металлических балок и железобетонного настила. Однако, при проектировании таких конструкций часто исходят из предпосылки, что стальная балка и железобетонная плита работают отдельно и не связаны друг с другом. Но в зарубежной практике и в ряде случаев, имевших место в России и в том числе в Республике Татарстан, в качестве перекрытия применяли сталежелезобетонные конструкции, запроектированные с учётом совместной работы стальной балки с железобетонной плитой.

Однако в целом сталежелезобетонные конструкции в отечественной практике не нашли должного распространения. Это, вероятно, связано с отсутствием нормативной базы и малой изученностью сталежелезобетонных перекрытий. Целью этой работы явилось проведение испытания фрагмента сталежелезобетонного перекрытия и получение экспериментальных данных напряженно-деформированного состояния для последующего их использования в разработке новых методик расчёта.

1. Экспериментальная установка.

В качестве фрагмента для испытаний изготовлено сталежелезобетонное перекрытие размерами 6000х6000 мм. Стальная часть перекрытия состоит из шести прокатных двутавровых балок № 20 по ГОСТ 8239-89 длиной 6000 мм, расположенных с шагом 1200 мм; бетонная часть: длина – 6000 мм, ширина – 6000 мм, высота – 80 мм. Армирование бетонной части производилось арматурными сетками из проволоки Ш5 Вр-I с шагом 100 мм по классической схеме для неразрезной балки. Совместность работы стальной и бетонной частей сталежелезобетонной конструкции достигалась за

счет двух рядов вертикальных анкерных стержней (2 Ш10 60 мм А-III), приваренных по всей длине к верхнему поясу стальных балок с шагом 150 мм в середине пролета, и 100 мм – по концам.

Применялся бетон класса В22,5 (М 300). Для определения его расчётных характеристик были изготовлены контрольные образцы – кубы 100х100х100 мм. При заливке монолитного бетона его уплотнение производилось глубинным вибратором.

Рис. 1. Вид опытной СЖБ плиты под нагрузкой

2. Измерительная аппаратура и методика замеров.

Для измерения деформаций стали и бетона на их поверхности наклеивались тензорезисторы с базой 50 мм (для бетона) и 20 мм (для стали). Продольные прогибы конструкции замерялись по центрам стальных балок с помощью линеек, укреплённых жестко на металлических треногах. Сдвиг по контакту сталь-бетон замерялся индикаторами часового типа с ценой деления 0,01 мм, укреплявшимися к концам стальных балок. Момент образования трещин и характер трещинообразования определяли визуально, а величина раскрытия трещин определялась с помощью микроскопа МБП-2 с 24-хкратным увеличением. Опытная разрушающая нагрузка фиксировалась путём предварительного определения веса всех грузов.

3. Результаты испытания.

Испытание проводилось постепенным нагружением однократной кратковременной статической нагрузкой сталежелезобетонной плиты перекрытия ступенями по 1/20 от ожидаемой разрушающей нагрузки. После каждого этапа нагружения снимались показания всех датчиков, индикаторов и прогибы.

При испытании изучался характер трещинообразования верхней и нижней граней железобетонной полки сталежелезобетонной плиты, а также закономерности развития деформаций бетона и стали несущих балок и монолитной плиты опытной сталежелезобетонной плиты.

Испытуемую плиту нагружали распределённой нагрузкой до 91 т. При нагрузке в 91 т прогиб конструкции составлял в разных зонах от 7,5 до 12 см, что составляет 1/50 длины конструкции (стальных балок). Таким образом, прогибы достигли недопустимых значений. При нагрузках от 0 до 91 напряжения продолжали наращиваться, происходило постепенное раскрытие продольных трещин в бетоне непосредственно над стальными балками, образовывалась сетка трещин в нижней части бетонной плиты, прогибы конструкции достигали 12 см, что означало наступление обеих групп предельных состояний.

При испытании опытной сталежелезобетонной плиты также изучались закономерности развития прогибов несущих балок фрагмента. Во всех шести несущих балках происходило увеличение прогибов при возрастании уровня нагружения, причем интенсивность их развития была различной на разных этапах.

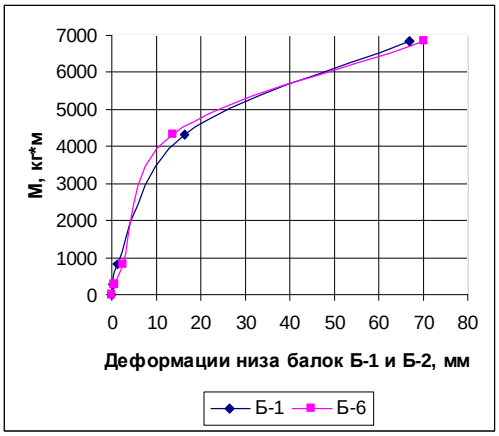

а)

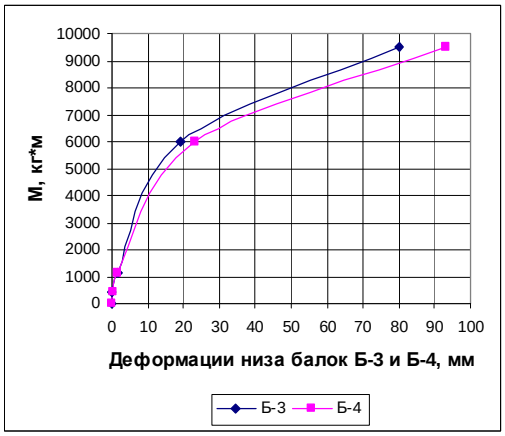

б)

Рис. 2. Деформации крайних фибр нижнего пояса стальной части, измеренные в зоне чистого изгиба на участке 60 см, для крайних (а) и средних (б) балок плиты

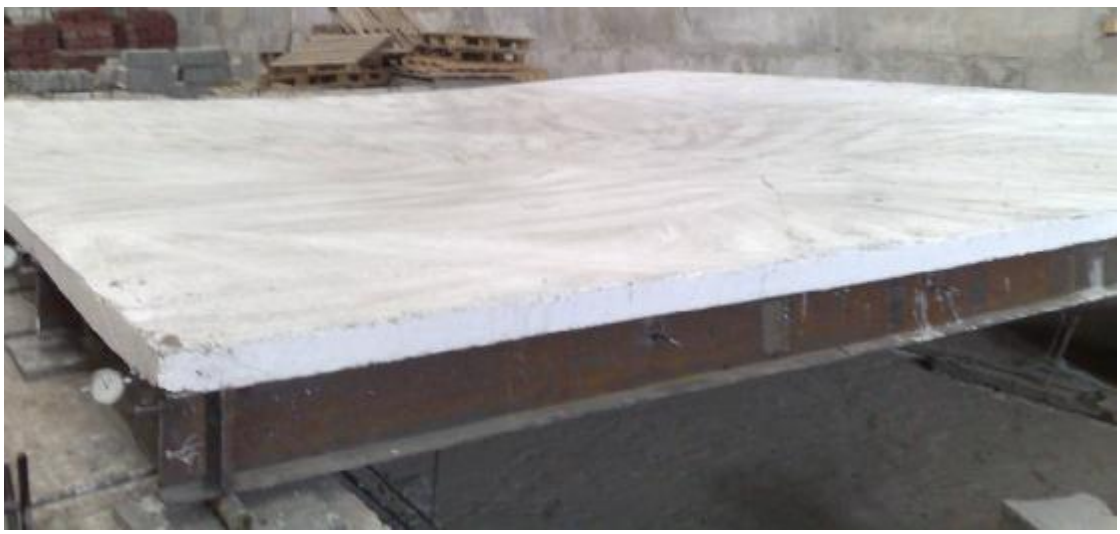

Рис. 3. Общий вид опытной сталежелезобетонной плиты после испытания

На начальных этапах загружения наблюдается практически прямая пропорциональность между изгибающим моментом и прогибами, а затем с изменением эпюры деформаций по высоте сталежелезобетонного сечения, вследствие появления неупругих деформаций стали, происходит интенсивный рост прогибов при незначительном увеличении нагружения, т.е. излом графика прогибов. Наличие изломов на графиках прогибов свидетельствует о снижении жесткости несущих балок сталежелезобетонного фрагмента при увеличении уровня нагружения.

Снижение жесткости несущих сталежелезобетонных балок происходит по растянутой зоне, вследствие снижения модуля упругости стали после того, как сталь сталежелезобетонного сечения входит в зону неупругих деформаций. Это объясняется сдерживающим влиянием неразрезной железобетонной плиты фрагмента сталежелезобетонного перекрытия, работающей в двух направлениях, и постепенным её включением в работу с увеличением уровня нагружения.

Наибольшее значение прогибов, а также наибольшие значения деформаций сжатия и растяжения в одинаковых сечениях по длине пролета достигались в средних (третьей и четвёртой) стальных балках опытной сталежелезобетонной плиты. Напряжения (деформации) нижних фибр стальной части сталежелезобетонного сечения развиваются более интенсивно, чем напряжения (деформации) по верхней грани бетонной полки, что свидетельствует о перераспределении усилий между сталью несущих балок и бетоном плиты и постепенном смещении нейтральной оси в сторону стальной части фрагмента сталежелезобетонного перекрытия.

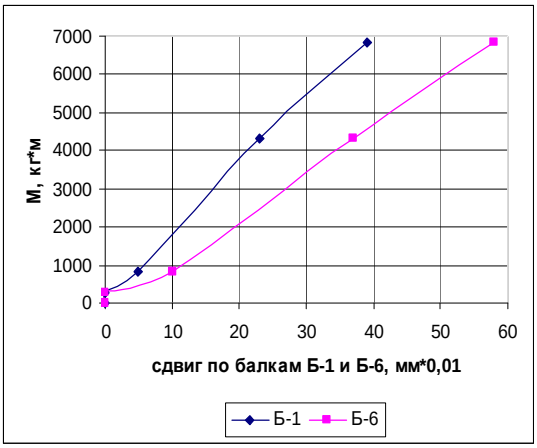

а)

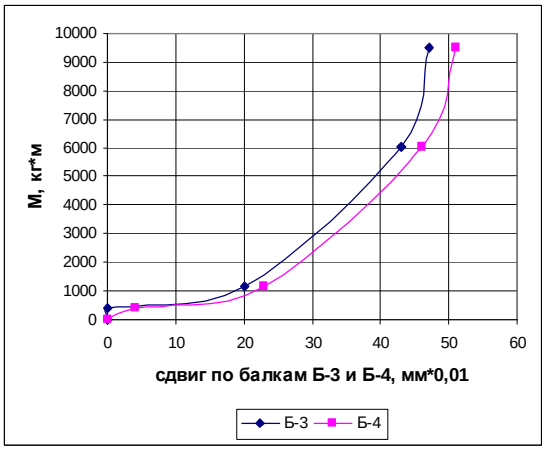

б)

Рис. 4. Графики развития максимальных деформаций абсолютного сдвига Δsh на границе контакта «сталь-бетон» для крайних (а) и средних (б) балок фрагмента перекрытия на различных этапах нагружения

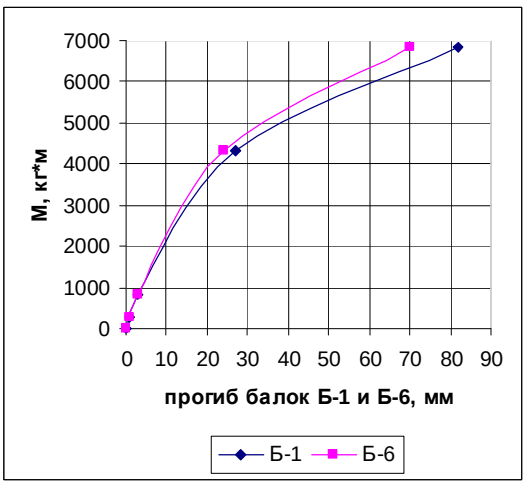

а)

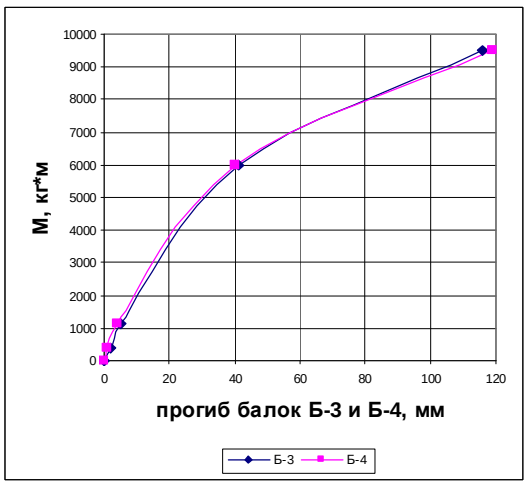

б)

Рис. 5. Графики развития прогибов в координатах «M-f» для крайних (а) и средних (б) балок фрагмента перекрытия на различных этапах нагружения

СПИСОК ЛИТЕРАТУРЫ

1. СНиП 2.05.03-84*. Мосты и трубы. – М.: Стройиздат, 1996. – 210 с.
2. СНиП 2.03.01-84*. Бетонные и железобетонные конструкции. Госстрой СССР. – М.: ЦИТП Госстроя СССР, 1989. – 80 с.
3. Замалиев Ф.С. Сталежелезобетонные конструкции. Новые методы расчета. – Казань, 1997. – 51 с.